Rock and Soil Mechanics

Volume 44 | Issue 1 Article 8

3-13-2023

Experimental study on immersion collapsibility process and vertical stress characteristics of large thickness loess foundation in Jingyuan area

De-ren LIU
School of Civil Engineering, Lanzhou Jiaotong University, Lanzhou, Gansu 730070, China

Zheng-shan AN
School of Civil Engineering, Lanzhou Jiaotong University, Lanzhou, Gansu 730070, China, 2805877360@qq.com

Shuo-chang XU
School of Civil Engineering, Lanzhou Jiaotong University, Lanzhou, Gansu 730070, China

Xu WANG
National and Provincial Joint Engineering Laboratory of Load & Bridge Disaster Prevention and Control, Lanzhou Jiaotong University, Lanzhou, Gansu 730070, China

See next page for additional authors

Custom Citation

LIU De-ren, AN Zheng-shan, XU Shuo-chang, WANG Xu, ZHANG Zhuan-jun, JIN Xin, ZHANG Yan, . Experimental study on immersion collapsibility process and vertical stress characteristics of large thickness loess foundation in Jingyuan area[J]. Rock and Soil Mechanics, 2023, 44(1): 268-278.

Experimental study on immersion collapsibility process and vertical stress characteristics of large thickness loess foundation in Jingyuan area

Authors

De-ren LIU, Zheng-shan AN, Shuo-chang XU, Xu WANG, Zhuan-jun ZHANG, Xin JIN, and Yan ZHANG

Rock and Soil Mechanics 2023 44(1): 268−278 ISSN 1000−7598
https: //doi.org/10.16285/j.rsm.2022.5266 rocksoilmech.researchcommons.org/journal

Experimental study on immersion collapsibility process and vertical stress characteristics of large thickness loess foundation in Jingyuan area

LIU De-ren[1], AN Zheng-shan[1], XU Shuo-chang[1], WANG Xu[1, 2], ZHANG Zhuan-jun[1], JIN Xin[1], ZHANG Yan[1]

1. School of Civil Engineering, Lanzhou Jiaotong University, Lanzhou, Gansu 730070, China
2. National and Provincial Joint Engineering Laboratory of Load & Bridge Disaster Prevention and Control, Lanzhou Jiaotong University, Lanzhou, Gansu 730070, China

Abstract: In order to study the water infiltration and self-weight collapse deformation characteristics of Jingyuan loess with large thickness under the condition of immersion, a field immersion test without water injection holes was carried out in the self-weight collapsed loess site of Jingyuan North Station along the Zhongwei–Lanzhou Railway. The surface and underground collapsible deformation, cracks, water content and vertical stress in the soil around the test pit were monitored and analyzed. The water diffusion, self-weight collapsible characteristics and vertical stress in the soil were studied, and the regional correction coefficient β_0 value and wetting angle were discussed. The results showed that: the change of volumetric water content was divided into four stages: immersion stabilization (two), rapid increase (one) and slow increase (one). In the immersion process, the vertical infiltration of water was accelerated and the radial diffusion was slowed down at 21 m, and the final shape of the wetting front was presented as elliptical. According to the water content test results of exploratory wells and boreholes, the maximum wetting angle was calculated to be 41°. The self-weight collapse process of loess in the site went through three stages: severe collapse, slow collapse and consolidation stabilization. At the end of the test, a total of 13 ring cracks were developed, and the farthest point of the cracks was 26 m from the edge of the test pit. According to the laboratory test and field test results, it was suggested that the regional correction coefficient should be corrected along the depth of the soil layer, and the β_0 value was taken as 1.05 within 0−10 m and 0.95 within 10−27 m. In the depth range from the surface to 21 m, the foundation soil was saturated and fully collapsed. The vertical stress in the soil increased linearly along the depth, and the vertical stress in the soil was close to the saturated self-weight stress. The foundation soil below 21 m failed to collapse entirely, and the vertical stress in the soil decreased gradually. The research results could be applied to the later construction of Zhongwei–Lanzhou Railway and provide a reference for other regional engineering projects.

Keywords: large-thickness loess foundation; water immersion test; collapse deformation; regional correction coefficient β_0; water diffusion; vertical stress in soil

1 Introduction

The formulation and implementation of China's *Medium-and Long-term Railway Network Plan* has effectively promoted the rapid development of railroad construction business in the northwest region[1], among which the construction of the Zhengzhou−Xi'an High-speed Railway, Baoji−Lanzhou High-speed Railway, and Lanzhou−Chongqing Railway has provided important support to deepen the two-way opening of land and sea and boost the coordinated development of the regional economy. With the increasing number of engineering projects in the loess area of northwest China, the construction sites are also transformed from loess low terraces to high terraces [2], and the consequent engineering construction problems keep emerging. As the most typical engineering characteristic of loess[3], the collapse has been widely concerned by people, and how to grasp the collapse deformation and immersion of large thickness self-weight collapse sites is a scientific problem that researchers need to solve urgently.

A large number of studies have been carried out by researchers on the loess collapse deformation pattern. Yang et al.[4] conducted collapse tests to investigate the factors affecting the collapse deformation of compacted loess under humidified conditions. Zheng et al.[5] revealed that the inhibitory effect of discontinuity in soil layer distribution on loess collapse deformation was the main reason for the discrepancy between the calculated value and the measured value of collapse based on the numerical calculation results. Shao et al.[6] described the microstructural changes of remodeled loess before and after collapse by electron microscopy, laser diffraction, and mercury intrusion porosimetry, and established a correlation between the microstructural evolution and the collapse behavior. Wei et al.[7] proposed that the

Received: 28 March 2022 Accepted: 25 April 2022
This word was supported by the National Natural Science Foundation of China (41662017).
First author: LIU De-ren, male, born in 1978, PhD, Associate Professor, Master supervisor, mainly engaged in the teaching and research work related to geotechnical engineering and special soil and cold zone engineering. E-mail: liuderen@mail.lzjtu.cn
Corresponding author: AN Zheng-shan, male, born in 1998, Master degree candidate, focusing on loess collapse. E-mail: 2805877360@qq.com

loess collapse was a result of the combined effect of microstructural and compositional characteristics by X-ray and scanning electron microscopy tests. Xu et al.[8] revealed the stress limit conditions of loess collapse deformation by triaxial immersion test. The above studies show that laboratory tests are an important method to study the collapse characteristics and collapse deformation of loess[3]. However, due to the different test conditions between laboratory and in situ immersion tests, the laboratory test can not truly reflect its collapse deformation development and immersion infiltration pattern when the thickness of the collapsible loess layer is large[9]. Therefore, it is particularly important to conduct in situ immersion tests to study the collapse deformation and immersion infiltration pattern of loess. Yuan et al.[10] carried out large-scale in situ immersion tests on the third terrace of the Wei River and the Xianyang loess tableland to evaluate the collapsibility of loess and proposed corresponding foundation treatment methods. Huang et al.[11−12] studied the self-weight collapse pattern, foundation treatment method and residual collapse amount of large thickness self-weight collapse loess by immersion pit experiments. Shao et al.[13] and Li et al.[14−15] conducted large field immersion tests on the ground surface above the loess tunnel to reveal the collapse deformation characteristics of the loess tunnel site and its degree of influence on the tunnel structure. Wu et al.[16] carried out large thickness self-weight collapse loess field immersion tests and conducted an in-depth study on two core problems of collapse and water infiltration characteristics of in-situ loess. Zhao et al.[17] investigated the water infiltration pattern during immersion and intermittent irrigation by the combination of field immersion tests and numerical calculations.

In summary, the research on loess collapse deformation has achieved rich results, and a large number of immersion tests have been carried out in Yuncheng, Shanxi Province; Ledu, Qinghai Province; Zhangjiakou, Hebei Province and Lanzhou, Gansu Province to study the loess collapse deformation and immersion infiltration pattern. However, the distribution of loess strata in different areas is heterogeneous and there is no obvious regional distribution pattern, and no relevant information on field immersion tests is available in Baiyin, Gansu Province. Based on this, relying on the large thickness collapse loess field of Jingyuan North Station along the Zhongwei−Lanzhou Railway, this study conducted in-situ pit immersion experiments to monitor the vertical settlement, water content, vertical stress in the soil and the development of cracks around the test pit during the process of immersion. The self-weight collapse deformation and immersion infiltration pattern under saturated and unsaturated conditions were studied. The research results would further provide reliable technical guidance and safety guarantee for the later design, construction and operation of the Zhongwei−Lanzhou Railway, and also provide valuable experience for the future large-scale engineering construction in this region.

2 Test overview

2.1 Engineering geological conditions of the test site

The test site is located on the loess high terrace on the north side of Mitan Town, Jingyuan County, Baiyin, with flat and open terrain. The elevation of the ground within the test site ranges from 1 463.61 to 1 464.93 m. Field samples were taken before the immersion test was carried out, and the basic physical property indexes of the loess in the area were obtained through laboratory tests, as shown in Table 1.

According to the field survey and engineering geological drilling data, the lithology of the strata in the test site is mainly the sandy loess of the Quaternary Holocene alluvial-pluvial deposit (Q_{4al+pl}) and the coarse rounded gravel soil and cobbly soil of the Quaternary Upper Pleistocene alluvial-pluvial deposit (Q_{3al+pl}). The engineering geological characteristics of each stratum are shown in Table 2.

2.2 Test pit design

According to the engineering geology conditions of the test site exposed by the exploratory wells, the large-scale field immersion test was conducted based on the *Standard for building construction in collapsible loess regions* (GB50025−2018)[3] in order to make the collapse soil layer below the bottom surface of the test pit saturated with water and fully produce self-weight collapse deformation. The test pit was circular, with a diameter of 24 m and a depth of 0.5 m. A 10 m thickness of sand and gravel was laid at the bottom of the pit.

A total of 73 settlement observation points were arranged in this experiment, among which 42 were shallow points and 30 were deep points. The numbers of test pit settlement monitoring points and exploratory wells are shown in Fig. 1.

Table 1 Basic physical and mechanical properties in natural condition

Depth /m	Initial water content w /%	Initial voild ratio e_0	Density ρ/(g • cm^{-3})	Liquidity index I_L	Plasticity index I_P	Cohesion c /kPa	Internal friction angle φ/(°)
0−10	20.433	1.025	1.417	0.253	10.271	9.290	21.856
11−20	21.833	1.112	1.360	0.250	9.803	10.005	29.982
21−30	21.200	0.981	1.441	0.263	9.946	10.396	36.791

Table 2 Lithological characteristics of the test site stratigraphy

Stratum No.	Stratum name	Stratum thickness /m	Stratum description
①	Sandy loess	21.0−37.3	Light yellow, mainly composed of silt particles, uniform with needle-like pores, sandy feeling when rubbed, slightly wet, slightly dense
②	Sandy loess	1.5−10.2	Light yellow, mainly composed of silt particles, uniform, sandy feeling when rubbed, wet, medium dense
③	Fine sand	0.5−1.6	Yellowish brown, mainly composed of quartz and feldspar, uneven sand containing a small amount of silt and clay particles, slightly wet, slightly dense, showing a transparent crystal distribution
④	Coarse rounded gravel soil	3.0−7.4	Greenish gray, mainly composed of sandstone and quartzite, rounded, wet, medium dense

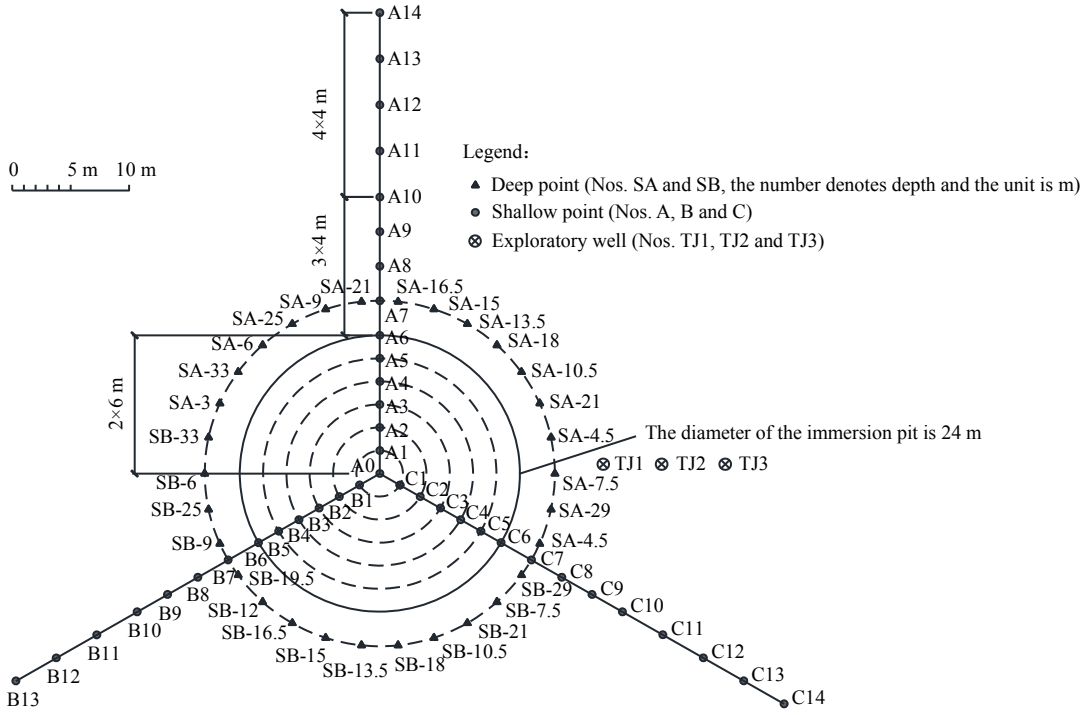

Fig. 1 Arrangement plan of test pit monitoring points

2.3 Shallow point arrangement

A shallow point (A0) was placed in the center of the test pit, the rest of the shallow points were arranged radially in three directions (A, B and C) from the center of the test pit to the outside of the pit at an angle of 120°. For the Line A, as an example, the layout spacing in each direction was: within the pit, 6 shallow points (A1−A6) were arranged at 2 m interval from the center of the test pit; outside the test pit, 4 shallow points (A7 to A10) were arranged at an interval of 3 m from 0 to 12 m from the edge of the test pit; 4 shallow points (A11 to A14) were arranged every 4 m from 12 m to 28 m from the edge of the test pit. The shallow point steel pipe was galvanized steel pipe, whose diameter was 0.025 m. The pipe length inside the test pit was 2.5 m, and the pipe length outside the test pit was 2.0 m. 0.15×0.15 m steel plates were set at the base of the shallow points in order to prevent the shallow points from falling due to the collapse of the loess surface and affecting the observation. The shallow pit for the base of the shallow point was manually excavated. After the shallow points were buried, the surrounding gap was backfilled and compacted.

2.4 Deep point arrangement

The deep points were arranged in a circumference of 15 m radius from the center of the test pit to observe the self-weight collapse of the soil layer at different depths. The adopted deep points were mechanical deep points, and the weight of the rod was approximately the same as the self-weight of the original overburden soil at the buried position. The depth setting principle was 2 deep points with equal depth set at an interval of 1.5 m from 3−21 m below 3 m from the pit bottom; 2 deep points with equal depth were set at every 4.0 m interval within 21−33 m; except at 3.0 m and 4.5 m where only one deep point was set, two deep points were set at the rest depths. There were a total of 30 deep points, and the plane spacing of each deep point was 2 m. The deep point device was composed of an inner pipe and an outer pipe. The inner pipe was used to measure the self-weight collapse of each soil layer. The galvanized steel pipe with a diameter of 0.025 m was used, and the base was a round PVC pipe with a height of 0.2 m and a diameter of 0.05 m, which was cast together with the galvanized steel pipe using concrete and located directly on the top surface of the

soil layer to be buried. The length of the inner pipe at each deep point was the corresponding borehole depth and then extended upward by 2 m, that is, the inner pipe was 2 m above the surface of the test pit. The outer pipe of the deep point adopted the PVC pipe with a diameter of 0.075 m, whose function was to protect the inner pipe to sink freely with the soil layer without being affected by the hole wall when each soil layer produced self-weight collapse. As the PVC pipe was exposed to the ground surface for 1 m, the gap between the outer pipe and the borehole was backfilled and compacted with plain soil.

2.5 Transducer arrangement

A total of 3 exploratory wells were excavated at 18, 23 m and 28 m from the center of the test pit. There were totally 28 moisture transducers, 20 pore water pressure transducers and 20 earth pressure cells buried in the three exploratory wells, and the specific buried locations are shown in Fig. 2. The moisture transducer, pore water pressure transducer and earth pressure cell were respectively the YH4800A, YH04-B and YH03-G models manufactured by Hunan Xiangyinhe Sensing Technology Co., Ltd. The embedding method was as follows. First of all, use the soil sampler knife to carve out a rectangular trough on the inner wall of the exploratory well, and the size and shape of trough were similar to the transducer; then put the transducer horizontally into the rectangular trough after labeled, fill the gap firmly with soil, backfill the exploratory wells with plain soil and compact in layers when all the transducers were embedded and could work normally; finally, fix the junction box on the ground surface in order to protect the transducer connector.

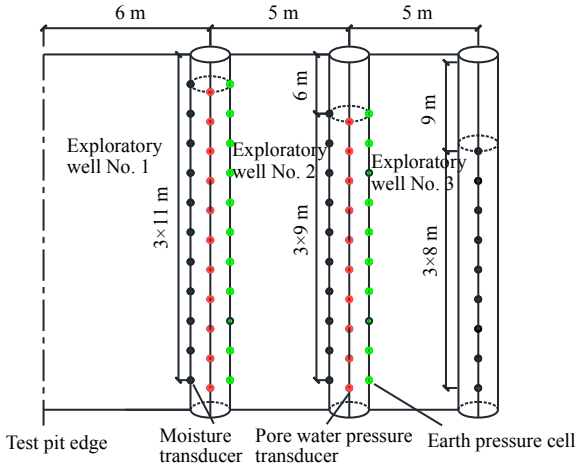

Fig. 2 Arrangement plan of transducers

2.6 Immersion test process

Figure 3 illustrates the photo of the field immersion test. The test lasted for 163 d, including immersion monitoring (March 24, 2021 to August 14, 2021) with a total of 12 908 m^3 water injection; 19 d of water cut-off (August 15, 2021 to September 2, 2021). During the immersion phase, the water head height was always maintained between 40 cm and 50 cm, while the data of settlement monitoring points and various sensing elements were recorded daily.

Fig. 3 Field photo

3 Analysis of water infiltration process

In this section, the variations of volumetric water content and water infiltration rate were investigated by the monitoring data of the exploratory well No. 1. The migration curve of the wetting front with time was plotted based on the time of water reaching the observation points at different depths in the three exploratory wells, and the maximum wetting angle of the test field was subsequently deduced from the variation of water content in the exploratory wells and boreholes.

3.1 Volumetric water content variation

In order to prevent excessive disturbance of the soil layer when the transducers were buried in the test pit, which would lead to deviation of the test results, three exploratory wells were placed outside the test pit to monitor the water infiltration, and the exploratory well No. 1 was the closest to the center of the test pit, so the volumetric water content monitoring data of the exploratory well No. 1 was used as an example for analysis.

As shown in Fig. 4, the volumetric water content monitoring data at the shallow (9 m), middle (18 m) and deep (33 m) depths of the exploratory well No. 1 were selected for analysis. Taking the depth of 9 m as an example, it could be seen that the change of volumetric water content during the immersion process was divided into four stages: stable immersion (*ab* and *de*), rapid increase (*bc*) and slow increase (*cd*). The stage *ab*: at the beginning of the immersion, the water did not reach the monitoring point, and the soil maintained the initial volumetric water content of 13.3%, which was basically unchangeable. The stage *bc*: at 38 d of the immersion, the water reached the depth of the monitoring point and the volumetric water content grew rapidly to 21.6%. The stage *cd*: after 60 d of the immersion, the volumetric water content increased slowly until the soil reached saturation. The stage *de*: at 138 d of the immersion, the volumetric water content tended to be stable and did not change.

In comparison, the variations of volumetric water content at 18 m and 33 m were almost the same as that

at 9 m. With the increase of depth, the longer the retention time of the stage *ab* at 18 m and 33 m, the later the time to enter the rapid increase stage. In the rapid increase stage, the volumetric water content increased by 7.4% at 9 m, 25.3% at 18 m, and 33.8% at 33 m. With the increase of depth, the variation of volumetric water content became more signifacant.

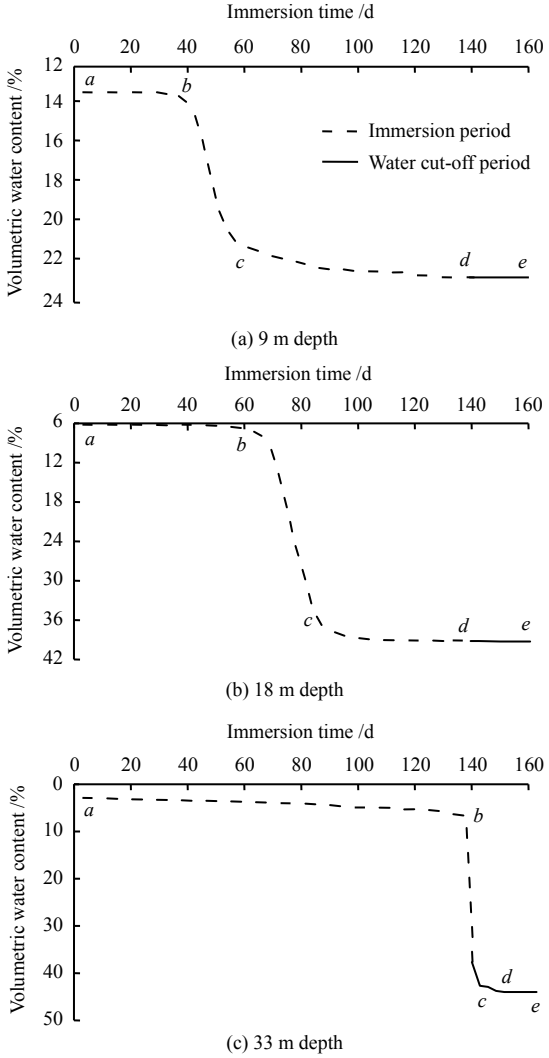

Fig. 4 Variation curves of volumetric water content of exploratory well No.1 at different depths

The water infiltration rates at different depths are shown in Table 3. The distance between two adjacent measurement points divided by the difference in the time of water migration at the two measurement points gives the mean infiltration rate of the soil layer at different depths[16]. Since there was no significant change in the volumetric water content at 3 m and the time for water to reach the observation point below 18 m was irregular, only the infiltration rate of the soil layer from 6 m to 21 m was considered.

According to Table 3, the infiltration rate at 6 m was the largest, which was 1.00 m/d, and the infiltration rate at 18 m was the lowest, which was 0.13 m/d. Overall, the infiltration rate gradually decreased along the depth, which was mainly because: (1) The deep soil was subjected to large overlying soil stress, the soil was more compacted, and with the collapse of shallow soil, the number of pores kept decreasing, leading to the difficulty of water infiltration. (2) The immersion process was a process of water-driven-air, as the water content in the pore increased, the air was not discharged in time to make the pore air pressure increase, preventing the downward migration of water.

Table 3 Water diffusion rates of loess at different depths

Depth /m	Arrival time of wetting front /d	Time for water content to reach the peak /d	Time difference /d	Infiltration rate /(m • d^{-1})
3	—	—	—	—
6	33	51	18	1.00
9	36	57	21	0.33
12	45	69	24	0.20
15	60	84	24	0.18
18	77	109	22	0.13
21	100	121	21	—

3.2 Development process of wetting front

Table 4 shows the time for water to reach the observation points at different depths in the three exploratory wells. From the table, it could be seen that as the depth increased, the time for water to reach the observation point was longer, but the water at 21−27 m did not conform to the top−to−bottom migration mode, and the water in the three exploratory wells reached 27 m first, taking 94, 106 d and 115 d, respectively. The reasons for the phenomenon were: (1) Loess had the characteristic of non-uniformity, the pore structure below 21 m was changed, the vertical infiltration rate of water increased and the radial diffusion decreased, the water did not reach the observation point at 21 m as a result. (2) With the infiltration of water, the air was gradually replaced by water, and the greater the depth, the more difficult it was for air to be discharged. The pore pressure increased to a critical value at 27 m, which restricted the downward infiltration of water and increased the radial diffusion, so that the water reached the observation point at 27 m first.

Table 4 Time required for the wetting front to reach each moisture meter observation point

Exploratory well No. 1		Exploratory well No. 2		Exploratory well No. 3	
Depth /m	Time /d	Depth /m	Time /d	Depth /m	Time /d
3	—	3	—	3	—
6	33	6	—	6	—
9	36	9	74	9	—
12	45	12	75	12	104
15	60	15	85	15	108
18	77	18	92	18	115
21	100	21	112	21	116
24	97	24	110	24	115
27	94	27	106	27	115
30	100	30	108	30	117
33	114	33	118	33	126

The migration time and distance relationship of the wetting front measured by the 28 moisture transducers are summarized in Fig. 5. It could be seen that the shape of the wetting front was smooth from 0 to 86 d,

it gradually spread along the vertical and radial directions with the increase of time, and the vertical infiltration accelerated when the water reached 21 m observation point; after 94 d of immersion, the water first reached 27 m in the exploratory well No. 1 and the wetting front was wide at the top and the bottom and narrow in the middle; after 128 d of immersion, the water reached all the observation points, and the final morphology of the wetting front resembled an ellipse (only the symmetric half was drawn in the figure), which had good similarity with the research results of Yao et al.[18] in the Lanzhou area.

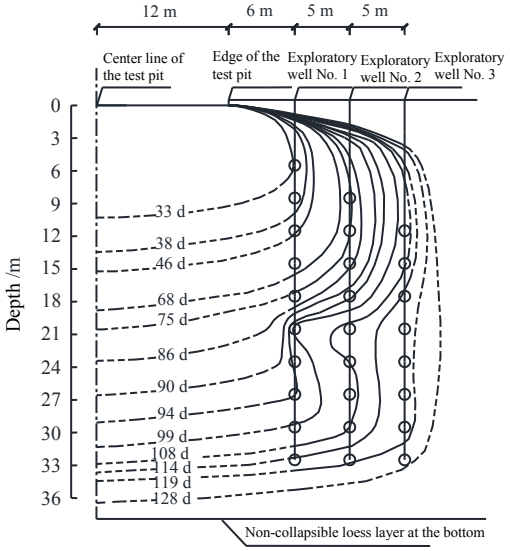

Fig. 5 Diffusion pattern profile of wetting front

After the immersion test, 2 exploratory wells at 26 m and 8 boreholes at 30 m were excavated for sampling to carry out laboratory tests, and the specific locations are shown in Fig. 6. Samples were taken at 2 m intervals in the boreholes for water content determination. The data from the east side were analyzed as an example, and the results are shown in Fig. 7.

As observated from Fig.7, the water content within the depth of 0−10 m (except the borehole No. 1) showed an overall increasing trend, and the water content within the depth of 10−30 m fluctuated between 14% and 18%.

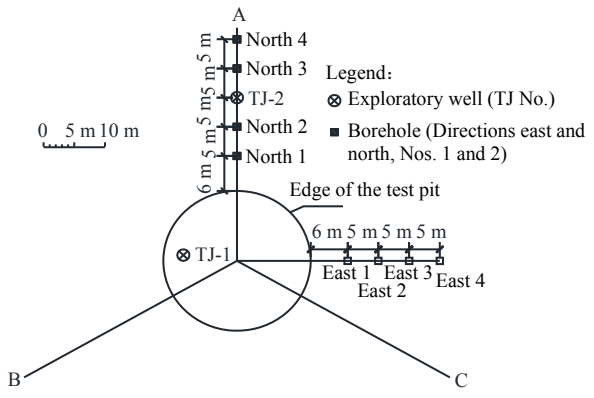

Fig. 6 Location map of exploratory wells and boreholes at the end of the test

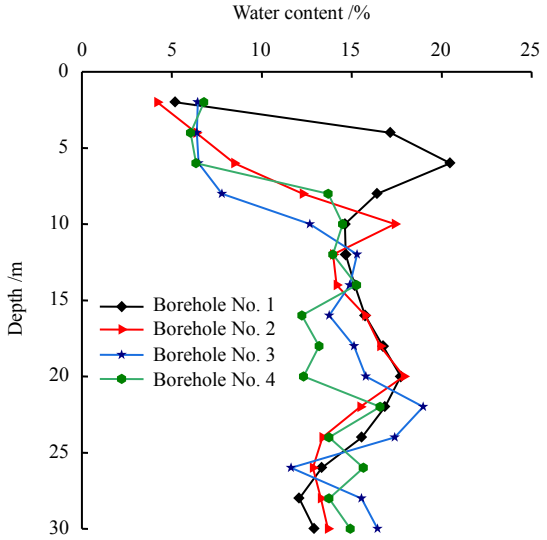

Fig. 7 Distribution of water content along the depth of each borehole

The maximum values were 20.5%, 17.9%, 18.9% and 16.6% in the boerholes No. 1, 2, 3 and 4 at depths of 6, 20, 22 m and 22 m, respectively. Since the borehole sampling was done 30 d after the end of immersion, the water continued to infiltrate along the vertical and radial directions during the water cut-off, resulting in an overall small water content.

3.3 Estimation of wetting angle

Yao et al.[18] found the wetting angle of a large thickness self-weight collapsed loess site in Lanzhou was 55° by the immersion test; Ma et al.[2] carried out the immersion test in the Jinzhong area and obtained a wetting angle of 45°; Wang et al.[19] determined the wetting angle was 42° by an immersion test of a collapsible loess site in Ledu, Qinghai. It could be seen that the wetting angle varied in different areas, and it was generally considered to be 45°, but the wetting angle deviated due to site conditions and soil layer properties.

The soil above the borderline of the wetting angle was never saturated. After the test, according to the water content of the exploration wells and boreholes, the soil at 3 m and 6 m of the exploration well No. 1; 9, 12 m and 33 m of the exploration well No. 2; and 12, 15, 18, 30 m and 33 m of the exploration well No. 3 was not saturated. The saturated and unsaturated regions are drawn, as shown in Fig. 8. The maximum wetting angle of the test site was deduced to be about 41°.

4 Collapse deformation results

4.1 Ground surface collapse deformation results

The test site was not equipped with water injection holes, the wetting process occurred gradually from shallow to deep layers, and the wetting process was slow and the period was long. At the end of the test, the ground surface settlement at the measurement point A0 in the center of the test pit was the largest, reaching 2.794 m; the ground surface settlement at the point A6 was the smallest, with 1.819 m. The settlement development

process of the measurement points A0 and A8 in the immersion test is shown in Figs. 9 and 10.

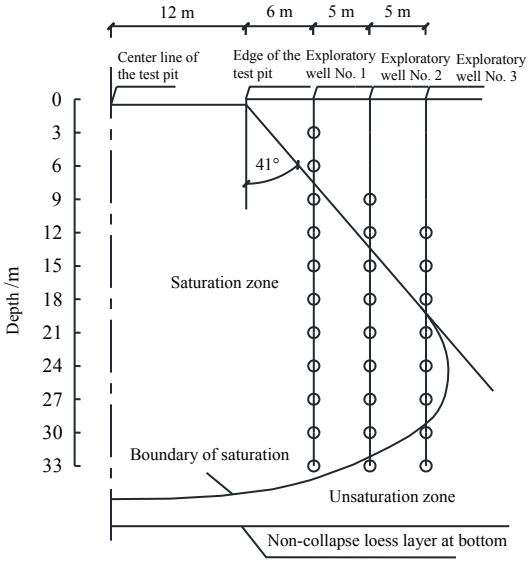

Fig. 8 Schematic diagram of saturated zone

A0 was taken as an example for the variation of the ground surface collapse in the test pit, and the variation of settlement for the rest settlement observation points was similar to it, so it would not be repeated here. Figure 9 shows the single-day and cumulative settlement variation curves of the measurement point A0. As could be seen from Fig. 9, the development of single-day settlement could be divided into three stages. The first stage (0−42 d) was the stage of severe collapse (single-day settlement ⩾0.03 m). The stage occurred at the beginning of immersion, where the water infiltrated downward through the pores, and the shallow soil was rapidly saturated, resulting in the failure of soil structure and the occurrence of dramatic settlement. The second stage (43−132 d) was the stage of slow collapse (0.005 m ⩽ single-day settlement < 0.03 m). With the increase of depth, the soil became more and more compacted, the infiltration of water slowed down, and the rate of collapse deformation decreased gradually. The third stage (133−162 d) was the stage of consolidation stabilization (single-day settlement <0.005 m). After the saturation and the collapse deformation of the upper soil, the settlement tended to be stable and the infiltration of water was difficult due to the increase of pore pressure. The mean daily settlement of this stage was less than 0.01 m and approached 0.001 m gradually.

The single-day settlement curve in Fig. 9 had three peak points A', B' and C', and the appearance of the peak point A' was related to the rapid failure of the soil structure and the large-scale settlement under the action of saturated self-weight stress; with the downward infiltration of water and the increase of vertical stress in the overburden soil, the lower soil could not withstand the large load, thus several collapse occurred, which made the single-day settlement increase again and reached the peak points B' and C'. The occurrence of the peak points in the single-day settlement variation curve was inferred to related to the multiple collapses in the large thickness loess site[18].

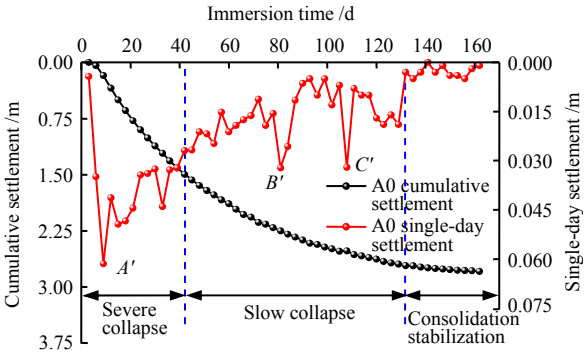

Fig. 9 Single-day and cumulative settlement process curves at measurement point A0

Figure 10 plots the ground surface single-day and cumulative settlement curves of the measurement point A8 outside the test pit. The development of single-day settlement could be divided into three stages: immersion stabilization (0−51 d), slow collapse (52−132 d) and consolidation stabilization (133−162 d). Unlike the ground surface collapse pattern in the test pit, the collapse deformation did not occur at the point A8 outside the test pit immediately after the immersion, reflecting an obvious “hysteresis effect”. This was because the pore pressure in the soil at the initial stage of immersion was small, the water continuously infiltrated downwards with less radial diffusion under the action of gravity. The water content of the soil at the point A8 did not reach the critical point of collapse deformation, therefore, there was no collapse deformation.

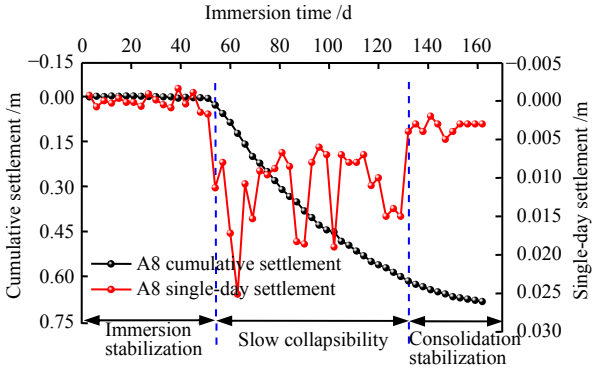

Fig. 10 Single-day and cumulative settlement process curves at measurement point A8

4.2 Deep collapsible deformation results

After 30 d of the test, the deep settlement of the test site was measured for the last time, and the data of 9 deep settlement observation points were selected and plotted in Fig.11. The settlement at the deep settlement observation point of 3 m reached 1.610 m and the settlement at 4.5 m reached 1.469 m. With the increase of depth, the cumulative settlement and the mean

settlement of each layer gradually reduced. The cumulative settlement at the observation points below 29 m was around 0.500 m, while the mean settlement of each layer also decreased from 0.094 m at 3.0 m to 0.013 m at 29.0 m. It showed that the settlement of deep loess became smaller and smaller, which also reflected the increasing difficulty of collapse for deep loess.

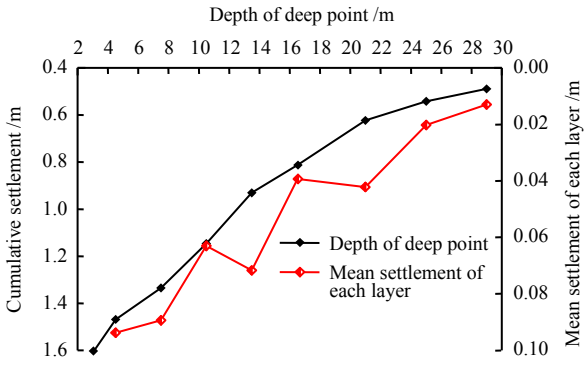

Fig. 11 Final settlement curves of deep settlement observation points

The variation of the deep settlement observation points was roughly the same as that of the ground surface settlement observation points. Fig. 12 plots the variation of the cumulative settlement at each deep settlement observation point. As the depth of the soil layer increased, the cumulative settlement deformation became smaller and smaller, and the starting point for the soil layer to enter the collapse deformation became later, which also reflected the obvious "hysteresis effect".

4.3 Surface crack development pattern

With the infiltration of water, the rapid failure of soil structure led to the occurrence of soil self-weight collapse deformation. Due to the different times and degrees of collapse deformation, it made the shear and tensile stress occur inside the soil, and thus resulting in cracks.

From the 4th day of immersion, the first crack appeared at the edge of the test pit. With the occurrence of self-weight collapse deformation of the soil layer, the cracks were continuously extended and eventually connected, forming a ring-shaped crack. The cracks expanded continuously from inside to outside, and a total of 13 ring-shaped cracks were generated at the end of the test, with the farthest crack being 26 m from the edge of the test pit, as shown in Figs. 13 and 14. The crack development lasted for 160 d, and the cracks no longer changed 2 d before the test was stopped.

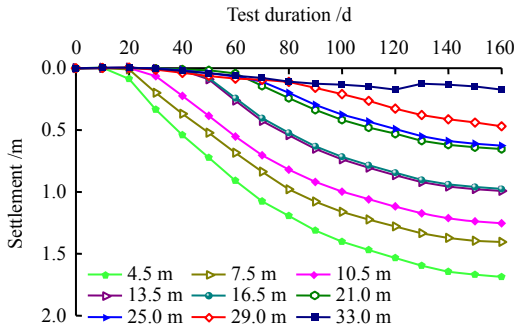

Fig. 12 Cumulative settlement variation process curves of deep settlement observation points

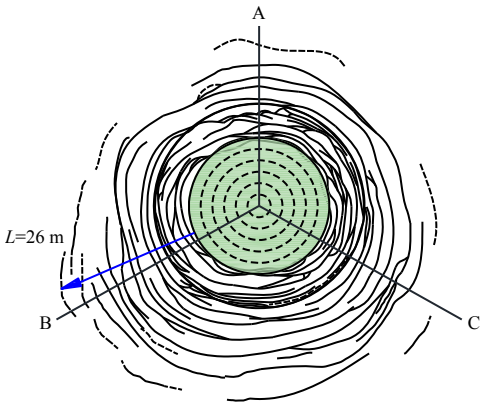

Fig. 13 Final shape of test pit cracks

Fig. 14 Final shape of field test pit cracks

4.4 Discussion of correction coefficient β_0

The loess in the Longxi area is widely distributed and the loess layer thickness is large. Many field immersion tests have been carried out, and the data of some field immersion tests in the Longxi area are summarized, as shown in Table 5.

Table 5 Statistic of immersion test in Longxi area

Test site	Soil layer thickness /m	Test pit diameter /m	Test pit size		Self-weight collapse /m		Regional correction coefficient β_0
			Length /m	Width /m	Measured	Calculated	
Donggang, Lanzhou	10.8	10	—	—	0.96	0.50	1.92
Xigu, Lanzhou	10.5	20	—	—	0.93	0.50	1.86
Heping, Lanzhou	36.5	40	—	—	2.32	1.23	1.89
Aluminum plant, Liancheng	18.0	—	55	55	1.15	0.54	2.13
Ershilipu, Tianshui	14.5	—	16	16	0.59	0.41	1.45
Fertilizer plant, Lucheng	10.0	15	—	—	0.25	0.18	1.35

It can be seen from Table 5 that the correction coefficient β_0 of the Longxi area was between 1.3 and 2.2, the correction coefficients in different areas had some differences, and there was no obvious distribution pattern. Therefore, it was very necessary to carry out field immersion tests to study the loess collapse before construction in different areas, considering factors such as engineering safety.

According to the collapsibility test, the collapsibility coefficient of self-weight for the soil layer at different depths was calculated. It was found that the collapsibility coefficient of loess self-weight increased with the depth, from 0.022 at 0 m to 0.086 at 27 m. The calculated results are shown in Table 6.

Table 6 Calculation table of correction coefficients for areas along the depth direction

Depth /m	Collapsibility coefficient of self-weight	Self-weight collapse /m		Regional correction coefficient β_0
		Calculated	Measured	
0	0.022	1.509	1.819	1.21
3	0.026	1.443	1.610	1.07
6	0.032	1.365	1.436	1.00
9	0.041	1.269	1.229	0.92
12	0.050	1.146	1.089	0.90
15	0.052	0.996	0.992	0.94
18	0.054	0.840	0.774	0.86
21	0.065	0.678	0.653	0.89
24	0.075	0.483	0.594	1.23
27	0.086	0.258	0.461	—

Based on the collapsibility coefficient of self-weight measured by laboratory tests, the self-weight collapse of the soil layer was calculated. The measured value of self-weight collapse was divided by the calculated value to obtain the value of the regional correction coefficient β_0 at different depths. Since the value of the regional correction coefficient β_0 varied greatly at different depths, it was suggested to be corrected along different depths of the soil, with the β_0 value of 1.05 for 0−10 m and the β_0 value of 0.95 for 10−27 m.

The ground surface regional correction coefficient β_0 was 1.21, which was less than the Longxi regional correction coefficient value of 1.50 in the *Standard for building construction in collapsible loess regions* (GB50025−2018)[3]. The reason for the above phenomenon was as follows: the test site was surrounded by paddy fields, the ground surface was irrigated by water all year round, and the partial collapse of shallow loess occurred in advance. As a result, the ground surface self-weight collapse amount measured by the test was small and the regional correction coefficient was low. Jingyuan North Station was close to the test site, and the lithological characteristics and ground surface conditions of the strata were basically the same. Therefore, the regional correction coefficient obtained from this test could provide a certain reference value for practical engineering.

5 Analysis of vertical stress in soil

Two exploratory wells were excavated at the test site and the earth pressure cells were embedded horizontally. Because the exploratory well No.1 was the closest to the center of the test pit, the vertical stress data in the soil of the exploratory well No. 1 was used as an example for analysis. Since the variation of vertical stress in the soil at different depths of the soil was slightly different, data from an observation point in each of the shallow (0−11 m), middle (12−22 m) and deep (23−33 m) layers of the test pit were selected to analyze the variation of vertical stress in the soil. The data from the observation points at the depths of 6, 12, and 27 m are plotted in Fig.15.

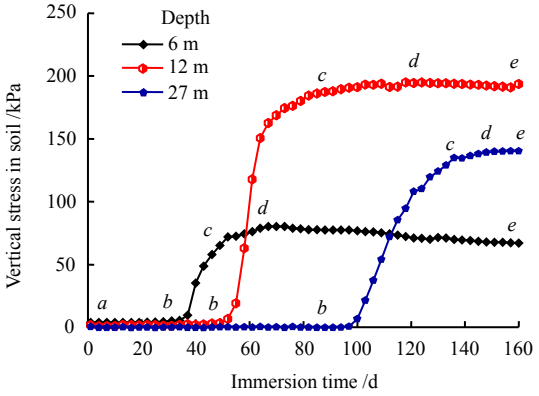

Fig. 15 Variation curves of vertical stress in test pit soil

One can see in Fig. 15, the vertical stress in the soil at different depths was close to 0 at the beginning of the test. This was mainly due to the fact that the earth pressure cells were horizontally placed in the trough of the exploratory well wall, and when the soil was not collapsed by water, the self-weight stress of the soil was borne by the undisturbed soil in the trough wall, the earth pressure cell basically did not bear the overburden soil stress. The vertical stress variation curve in the soil could be roughly divided into 4 stages: 2 stationary stages (*ab* and *de*), 1 rapid increase stage (*bc*) and 1 slow increase stage (*cd*). The stage *ab*: the vertical stress in the soil remained almost stable, the water did not reach the observation point and the upper soil was immersed but no collapse deformation occurred. The stage *bc*: the vertical stress in the soil increased rapidly, which indicated that the upper soil was saturated after immersion and self-weight collapse deformation occurred, implying that the self-weight stress of the upper soil had transferred to the observation point. The stage *cd*: as the collapse deformation of the upper soil occurred continuously, the vertical stress in the soil increased slowly, and the vertical stress in the soil reached the maximum value after the upper soil fully collapsed. The stage *de*: the vertical stress in the soil remained stable without change (except at 6 m), indicating that the upper soil completely collapsed.

It is generally accepted that the vertical stress in

soil increases with the increase of depth. By comparing the variations of the vertical stress in the soil at 6 m and 12 m, it could be found that the vertical stress in the soil at 6 m entered the rapid increase stage earlier, which was in accordance with the pattern of self-weight collapse deformation for soil from top to bottom, and the curve slope was very steep at the stage of rapid increase at 12 m. However, by comparing the variation curves of vertical stress in the soil at 12 m and 27 m, it was found that the increase range of vertical stress in the soil at 27 m was small, which did not conform to the pattern that the vertical stress in soil increased with the increase of depth. The reasons for this phenomenon might be as follows: the soil was saturated with water, resulting in collapse deformation, however, the collapse deformation of the soil near the observation point of 27 m was insufficient, so that the vertical stress in the overburden soil could not be transferred to the observation point completely. As a result, a small value of the vertical stress was captured at the observation point.

The data measured by the 11 earth pressure cells in the exploratory wells No.1 are illustrated in Fig. 16, and the unit weight of the loess layer at the test site calculated through the laboratory test was 16 kN/m^3. From the figure, the vertical stress in the soil within 0−20 m depth was close to the bound of the saturated self-weight stress except at 9 m. The maximum value of vertical stress in the soil at 21 m was 335.4 kPa, indicating that the soil layer above 21 m reached saturation during immersion and the collapse deformation was sufficient. The vertical stress in the soil at 9 m was small, which might be caused by uncompacted backfilling when the earth pressure cell was installed at 9 m. The vertical stress in the soil from 21 m to 33 m stayed off the bound of the saturated self-weight stress. However, the analysis of water infiltration showed that the soil from 6 m to 33 m in the exploratory well No.1 was saturated.This phenomenon could be explained by the fact that the soil below 21 m was not fully collapsed, so that the vertical stress in the upper soil could not be transferred to the observation point normally, resulting in a small value of vertical stress in the soil at the observation point.

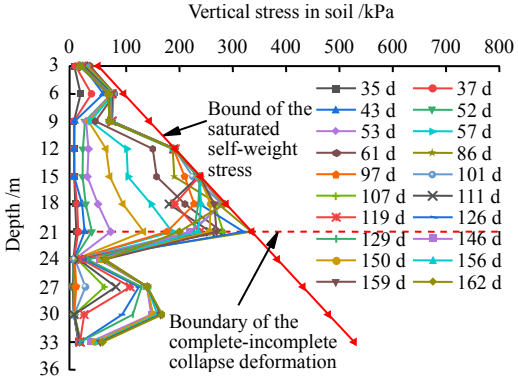

Fig. 16 Variation curves of vertical stress in soil at different depths of exploratory well No.1

The above analysis suggested the depth of 21 m was the boundary of the complete−incomplete collapse deformation of the soil layer. The soil layer above 21 m was fully collapsed and deformed, the vertical stress in the soil increased linearly along the depth, and the maximum value of vertical stress in the soil at 21 m was 335.4 kPa, which was close to the saturated self-weight stress. The soil layer below 21 m was saturated by water but the collapse deformation was not sufficient, and the overall vertical stress in the soil was small.

6 Conclusion

In this paper, a combination of laboratory test and immersion test was used to conduct an in-depth research and analysis on the infiltration and self-weight collapse characteristics of large thickness collapsible loess in the Jingyuan area. The following conclusions are drawn.

(1) The collapse deformation patterns of the ground surface and deep layer in the site were similar, and three stages, i.e., severe collapse, slow collapse and consolidation stabilization were identified. It was found that the further away from the center of the test pit, the later the collapse deformation occurred by comparing the two shallow points A0 and A8. As the depth of the soil layer increased, the cumulative settlement became smaller and smaller, and the soil layer took longer to enter the severe settlement, all reflecting an obvious “hysteresis effect”.

(2) A total of 13 ring-shaped cracks were developed at the end of the test, and the farthest crack was 26 m away from the edge of the test pit. According to the results of laboratory and field tests, it was recommended that the regional correction coefficient should be corrected along the different depths of the soil layer, with the β_0 value of 1.05 within 0−10 m and the β_0 value of 0.95 within 10−27 m.

(3) The variation of volumetric water content could be classified into four stages: immersion stabilization (two), rapid increase (one) and slow increase (one). In the process of immersion infiltration, the water infiltration accelerated at 21 m, and the final shape of the wetting front was similar to an ellipse. Based on the results of water content tests in the exploratory wells and boreholes, the maximum wetting angle of the test site was deduced to be about 41°.

(4) In the depth range from the ground surface to 21 m, the loess layer was saturated and fully collapsed. The vertical stress in the soil increased linearly with depth, reaching 335.4 kPa at 21 m. The vertical stress in the soil was close to the saturated self-weight stress, and the loess layer below 21 m failed to collpase sufficiently, and the vertical stress gradually decreased.

References

[1] WANG Meng-shu, An overview of development of railways, tunnels and underground works in China[J]. Tunnel Construction, 2010, 30(4): 351−364.

[2] MA Yan, WANG Jia-jing, PENG Shu-jun, et al. Immersion tests on characteristics of deformation of self-weight collapsible loess under overburden pressure[J]. Chinese Journal of Geotechnical and Engineering, 2014, 37(3): 537−546.

[3] Ministry of Housing and Ubran-Roral Department of the People's Republic of China. GB50025－2018 Standard for building construction in collapsible loess regions[S]. Beijing: China Construction Industry Press, 2018.

[4] YANG Yu-sheng, LI Jing, XING Yi-chuan, et al. Experimental study on moistening deformation characteristics of compacted loess and their influencing factors[J]. Chinese Journal of Geotechnical Engineering, 2017, 39(4): 626−635.

[5] ZHENG Jian-guo, DENG Guo-hua, LIU Zheng-hong, et al. Influence of discontinuous distribution of collapsible loess on its deformation[J]. Chinese Journal of Geotechnical Engineering, 2015, 37(1): 165−170.

[6] SHAO X X, ZHANG H Y, TAN Y. Collapse behavior and microstructural alteration of remolded loess under graded wetting tests[J]. Engineering Geology, 2018, 233: 11−22.

[7] WEI Y N, FAN W, YU B, et al. Characterization and evolution of three-dimensional microstructure of Malan loess[J]. Catena, 2020, 192. https://doi.org/10.1016/j.catena.2020.104585

[8] XU Ping, MIAO He-chao, SHAO Sheng-jun, et al. Research on wetting and collapsible deformation characteristics of collapsible loess under different triaxial stress conditions[J]. Chinese Journal of Applied Mechanics, 2021, 38(5): 1966−1973.

[9] SHAO Sheng-jun, LI Jun, LI Guo-liang, et al. Evaluation method for self-weight collapsible deformation of large thickness loess foundation[J]. Chinese Journal of Geotechnical Engineering, 2015, 37(6): 965−978.

[10] YUAN Q L, LONG S D, WEN F. Loess collapsibility characteristics of railway engineering sites using large-scale trial immersion pit experiment[J]. Bulletin of Engineering Geology and the Environment, 2021, 80(4): 3271−3291.

[11] HUANG Xue-feng, ZHANG Guang-ping, YAO Zhi-hua, et al. Research on deformation, permeability regularity and foundation treatment method of dead-weight collapse loess with heavy section[J]. Rock and Soil Mechanics, 2011, 32(Suppl.2): 100−108.

[12] HUANG Xue-feng, LIU Chang-ling, YAO Zhi-hua, et al. Study of infiltration and collapsible deformation law of unsaturated loess under over burden pressure by using TDR soll water probe[J]. Chinese Journal of Rock Mechanics and Engineering, 2012, 31(Suppl.1): 3231−3238.

[13] SHAO Sheng-jun, LI Jun, LI Guo-liang, et al. Field immersion tests on tunnel in large-thickness collapsible loess[J]. Chinese Journal of Geotechnical Engineering, 2018, 40(8): 1395−1404.

[14] LI Jun, SHAO Sheng-jun, LI Guo-liang, et al. Collapse deformation of loess tunnel and its effect[J]. Chinese Journal of Rock Mechanics and Engineering, 2018, 37(1): 251−260.

[15] LI J, SHAO S J, SHAO H. Collapsible characteristics of loess tunnel site and their effects on tunnel structure[J]. Tunneling & Underground Space Technology, 2019, 83: 509−519.

[16] WU Xiao-peng, WANG Lan-ming, FANG Jian-hong, et al. Seepage characteristics and their relationship with self-weight collapse of intact loess ground[J]. Chinese Journal of Geotechnical Engineering, 2018, 40(6): 1002−1010.

[17] ZHAO Zhi-qiang, DAI Fu-chu, MIN Hong, et al. Research on infiltration process in undisturbed loess-paleosol sequence[J]. Rock and Soil Mechanics, 2021, 42(9): 2611−2621.

[18] YAO Zhi-hua, HUANG Xue-feng, CHEN Zheng-han, et al. Comprehensive soaking tests on self-weight collapes loess with heavy section in Lanzhou region[J]. Chinese Journal of Geotechnical Engineering, 2012, 34(1): 65−74.

[19] WANG Xiao-jun, MI Wei-jun, XIONG Zhi-wen, et al. Water immersion field tests of collapsibility of loess foundation of Zhengzhou-Xi'an passenger dedicated line[J]. Journal of the China Railway Society, 2012, 34(4): 83−90.